

# High-Temperature (940 °C) furnace in 18/20 T cold bore magnet

HPSTAR  
536-2018



Ze Wang<sup>a,1</sup>, Yubin Hou<sup>a,b,1</sup>, Qiyuan Feng<sup>a,b</sup>, Hongliang Dong<sup>d</sup>, Qingyou Lu<sup>a,b,c,\*</sup>

<sup>a</sup> High Magnetic Field Laboratory, Chinese Academy of Sciences and University of Science and Technology of China, Hefei, Anhui 230026, People's Republic of China

<sup>b</sup> Hefei National Laboratory for Physical Sciences at Microscale, University of Science and Technology of China, Hefei, Anhui 230026, People's Republic of China

<sup>c</sup> Collaborative Innovation Center for Artificial Microstructure and Quantum Control, Nanjing 210093, People's Republic of China

<sup>d</sup> Center for High Pressure Science and Technology Advanced Research, Shanghai 201203, People's Republic of China

## ARTICLE INFO

### Keywords:

Furnace  
LN<sub>2</sub> jacket  
Cold bore magnet  
Cobalt oxide nanoparticle

## ABSTRACT

We present a high-temperature furnace that can work continuously in an 18/20 T cold bore magnet. A specially designed liquid nitrogen (LN<sub>2</sub>) jacket is between the high-temperature parts of the furnace and the liquid helium in the magnet Dewar. With LN<sub>2</sub> serving as the cooling medium, the calculated value of radiation received by the liquid helium (LHe) is as low as 0.004 W. The furnace can be put into LHe Dewar directly. Together with the magnet, the furnace can provide experimental conditions of a strong static magnetic field and temperatures up to 940 °C. A cobalt oxide synthesis in solution was carried out at 200 °C with and without a 15 T magnetic field for 8 h. Differences in material structure with the applied field were observed in transmission electron micrographs of the products. A Co film sample was treated at 900 °C with and without a 6.8 T magnetic field for 30 min. The scanning electron micrographs of the treated samples show that magnetic field had a clear effect on the heat treatment process. These two applications confirmed the performance of the furnace both in high magnetic field and at high temperature.

## 1. Introduction

As fundamental physical parameters, both magnetic field and temperature can influence some important processes in nature. The combination of a magnetic field and high temperature have been proved valuable for studying phenomena such as crystal growth, grain boundary development, and phase transitions. Before the invention of superconducting magnets, a uniform magnetic field was achieved using resistive electromagnets. Recrystallization of iron–cobalt alloys in a magnetic field applied by an electromagnet was studied as early as 1949 [1]. Resistive electromagnets have difficulty reaching field strengths above 1 T because of Joule heating of the coil. Stronger magnetic fields generated by superconducting magnets made it possible to observe the effect of magnetic fields on nonmagnetic alloy systems [2,3]. During the research boom of high-temperature superconducting (HTSC) materials in the late 1980s and early 1990s, application of a magnetic field during sample growth or treatment was proposed as a method to increase the critical current. To enhance the anisotropy of samples, strong magnetic fields (9.4 T) were applied to certain HTSC materials [4–6]. Considerable grain alignment was achieved in YBCO and HoBCO [5] by applying magnetic fields during their sintering

processes. Improved performance of Bi-based HTSC materials induced by a magnetic field was achieved by Pavard et al. [7,8]. In addition to alloys and HTSC specimens, magnetic fields also influence the growth of various other materials, such as Fe<sub>3</sub>O<sub>4</sub> crystal nanowires [9,10], carbon fibers [11], and hydroxyapatite [12].

In most applications, use of a higher strength magnetic field can lead to a stronger effect. For example, in the magnetic annealing of YBa<sub>2</sub>Cu<sub>3</sub>O<sub>7</sub> [13] and SmCo [14], the anisotropy energy is proportional to the square of the field value. This energy characterizes the ability of particles to crystallize along the field orientation against the thermal disordering effect.

The magnetic fields used in above applications were provided by room-temperature bore superconducting magnets. The drawback to this method is the use of bore volume for thermal insulation, consisting first of a region between the high-temperature furnace and room temperature, which typically involves a water-circulating cooling jacket, and a second region between room temperature and the cold magnet. The functions of these two subsystems overlap to some extent, so this does not provide a compact structure for the whole system. The strongest magnetic field that can be applied to a furnace is 12 T in this type of system, as far as the authors can find.

\* Corresponding author at: High Magnetic Field Laboratory, Chinese Academy of Sciences and University of Science and Technology of China, Hefei, Anhui 230026, People's Republic of China.

E-mail address: [qxlu@ustc.edu.cn](mailto:qxlu@ustc.edu.cn) (Q. Lu).

<sup>1</sup> Ze Wang and Yubin Hou contributed equally to this work.

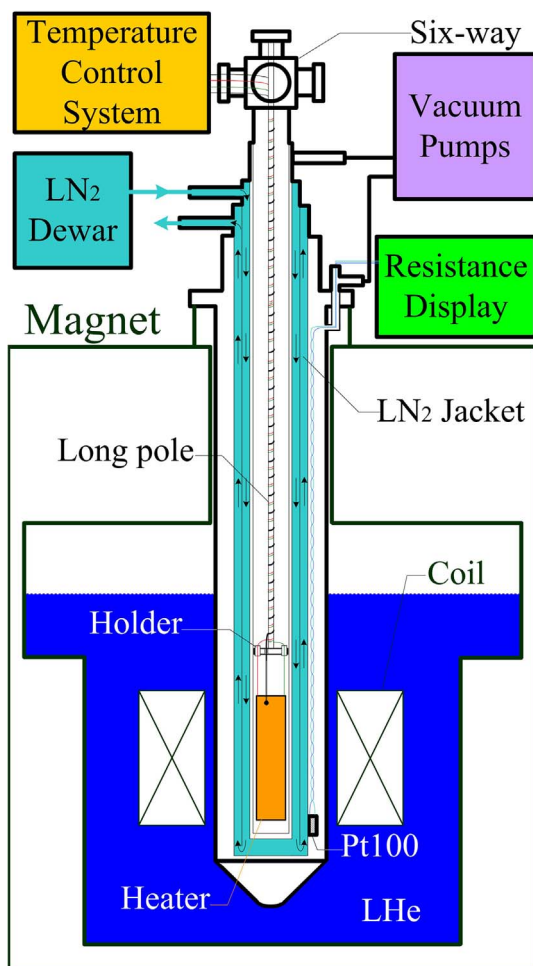


Fig. 1. Schematic of the furnace system within a cold bore superconducting magnet, showing the five-tube shielding system and its connections to other important components.

Instead, directly creating a high-temperature area in cold bore of a superconducting magnet optimizes the volume because no extra room is wasted for the nonessential room-temperature area. As a result, this architecture increases the furnace volume and the maximum field that can be applied.

The greatest challenge to designing furnaces in cold bore magnets is limiting heat conduction and radiation in such restricted space. In our new furnace system, a LN<sub>2</sub> jacket was designed to solve this problem (Fig. 1). The most important function of the jacket is to absorb heat radiation. Low temperature can also contribute to suppressing degassing, such that better vacuums inside and outside the jacket can be achieved. This is helpful to improving the efficiency of heat-conduction isolation. The jacket can also serve as a cold source, making sample treatments like cooling to low temperature (−60 °C, for example) and fast cooling possible. Compared with furnaces in room bore superconducting magnets, our furnace makes better use of space and can work at stronger magnetic field. Compared with furnaces in water-cooled magnets [15], our furnace can have lower running costs.

This paper describes the design and performance of this new type of furnace. The furnace structure provides a reference for designing high-temperature experiments in a liquid helium (LHe) environment.

## 2. Mechanical parts

A schematic of the furnace system in the magnet is given in Fig. 1, showing components: the heater, temperature control system, furnace chamber etc.

Detail of the heater is shown in Fig. 2. The electric heater comprises a 50.4 cm long corundum tube and Ni-Cr heating wire in the sidewall of the tube. Inner diameter of the long corundum tube is 12.6 mm. A K-type thermocouple is used to monitor and control the furnace temperature, which can be adjusted from −80 °C to 999 °C. 47 mm high special-designed tubes made of corundum are used for treating more samples in one experiment. These tubes have a 12.5 mm outer diameter (Fig. 2e) and they are divided into three parts, to accommodate of three samples. The sample tubes can be put into the long corundum directly (Fig. 2c). The small hole in the center of the sample tube is designed for connecting different sample tubes via a wire, making it convenient to put into (out of) the long corundum tube. A six-way cross, which has six KF40 flange ports, is on the top the furnace chamber. One of its horizontal flanges is used for connections for electrodes of thermocouple

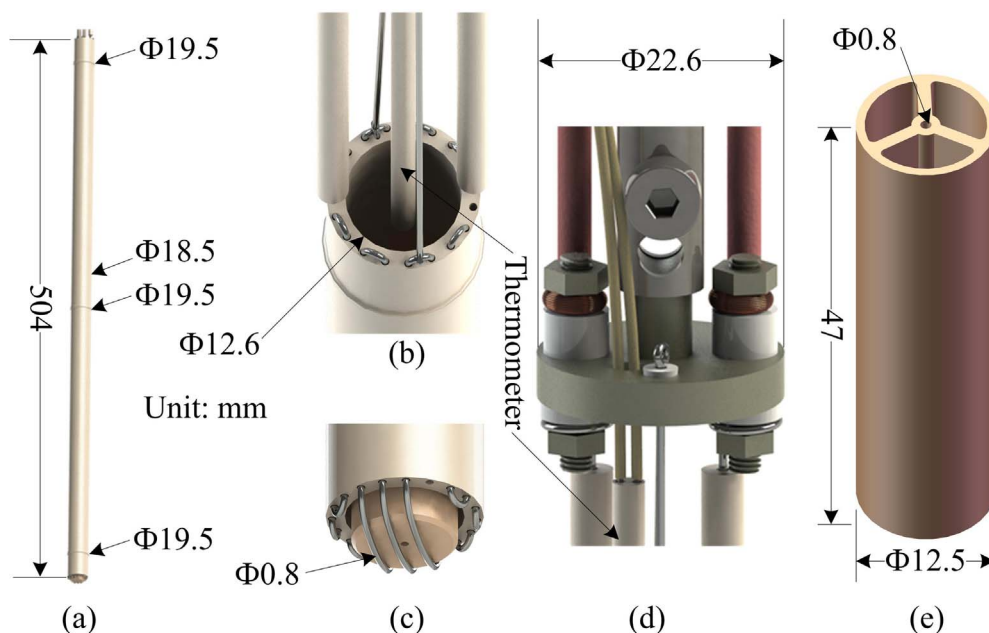


Fig. 2. Details of the heater. (a) Design picture of the long corundum tube, with detail of its (b) top and (c) bottom regions, (d) picture showing connections with the holder, and (e) three-dimensional schematic of corundum tube designed for samples.

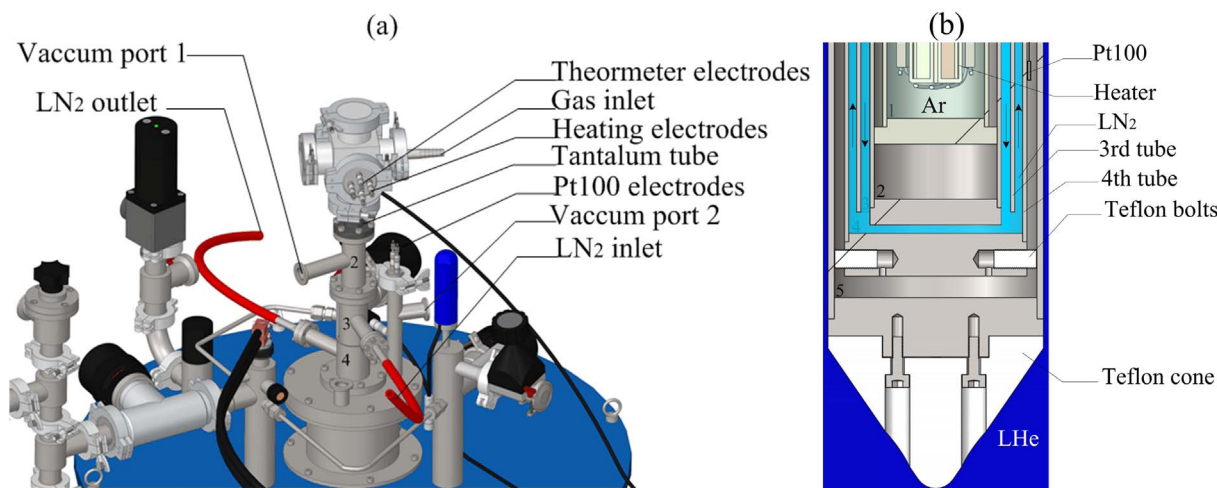


Fig. 3. Detail of the (a) top and (b) bottom of the furnace chamber. The former is a three-dimensional design image and the latter is a sectional drawing.

and heating wires. On the bottom of its upper vertical flange, a long stainless steel pole in diameter of 8 mm is welded (Fig. 1). The pole is used for fixing wires. A tantalum holder (Fig. 2d) is fixed on the bottom of the pole. The holder is used to hang the heater and it has a distance of 0.33 m from the long corundum tube. The distance is designed to make the holder have a temperature much lower than the heater. This is important because it reduces the heat loss and makes sure that the copper wires at the junctions on the holder will not melt. Six small sapphire bushings (white parts in Fig. 2d) serve as electric insulators for the hanging wires. Two of the hanging wires are connected to the copper wires electrically through tantalum bolts. These two wires are protected by corundum sheaths with inner diameter of 1.2 mm.

Fig. 3 shows detail of the top and bottom of the furnace chamber. Five long rolled and finished metal tubes form a heat shielding system aimed at protecting the long corundum tube from cooling by the LHe and thereby ensure its acceptable consumption rate. These tubes are labeled in order of increasing radius, as shown in Fig. 3. Neighboring tubes are connected by an ISO flange, making them removable from each other and the gaps between them sealable for creating a vacuum. The exception is the link between third and fourth tubes, which are welded together. There are four ISO flanges in the furnace-magnet system. In three flanges, Fluororubber O rings are used for sealing because of their better performance (compared with normal rubber) at temperatures below 0 °C. The flange connecting the fourth and fifth tubes is sealed by a 2 mm Indium wire in order to maintain good sealing performance during long running times of the furnace. The first tube, which is the thinnest, is made of tantalum; the other tubes are made of stainless steel. Tantalum was chosen mainly because of its good machinability and high stability in argon atmosphere below 1700 °C [16]. A turbo pump creates a vacuum in the gap between the first two metal tubes; a similar vacuum is created between the last two tubes. The vacuums reduce heat exchange between the sets of tubes. An LN<sub>2</sub> jacket, formed by the second, third, and fourth steel tubes, is designed to absorb radiation from the tantalum tube. The jacket also improves the vacuums and it is helpful to maintain a stable high furnace temperature. Unlike the others, the third tube does not have a round plate welded to its bottom (Fig. 3(b)), to allow continuous flow of LN<sub>2</sub>. The function of the third tube is to make sure that LN<sub>2</sub> can reach the bottom of the jacket. The LN<sub>2</sub> is provided from a 200 L self-pressurized Dewar, which enables the flowrate to be adjusted. The spaces inside and outside the third tube have the same cross-sectional areas, minimizing the total flow resistance. Paper and aluminum foil are rolled around the thickest tube of the jacket: the paper helps to insulate heat conducting to the foil, and the foil reduces radiation of the LN<sub>2</sub> because of its low emissivity. A platinum resistance (Pt100) ensures that the LN<sub>2</sub> flow is

continuously visible when the furnace is working. A Teflon cone is fixed on the bottom of the fifth tube (diameter of 50.8 mm), making it easier to insert the furnace into the magnet. By adding a simple adapter designed for other magnets, this system can be fitted to any type of magnet with a bore diameter of at least 52 mm.

The biggest difficulty in manufacture is the fracture problem of the 19-hole long corundum tube in its fabrication. The long tube has a small thickness at the edges of the holes, which can cause fracture problems in the sintering process. Another difficulty is finding the material to manufacture the first tube. We found stainless steel 304 deformed and caused carbon containment when the temperatures were above 600 °C in our earlier experiments. We also tried Ni-Cr alloy tube, but it melted at the point where it touched the long corundum tube when the furnace was heated to 970 °C. We chose tantalum at last because it has higher melt point and better corrosion resistance than Ni-Cr alloys.

### 3. Temperature control system

A schematic of the temperature control system is shown in Fig. 4. The system controls the temperature by adjusting on-off time spacing of the heating circuit. The heating circuit consists of the heater, a commercial 155 V DC power supply, and a DC-controlled solid-state relay (SSR). The PID circuit controls the on-off state of the heating circuit

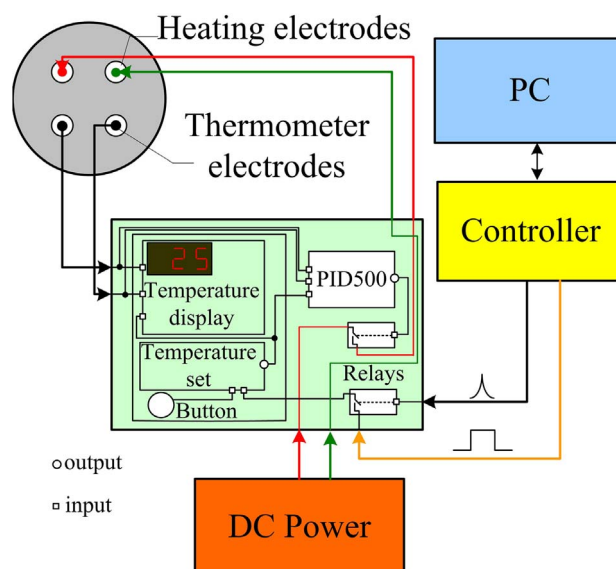


Fig. 4. Schematic of temperature controlling system.

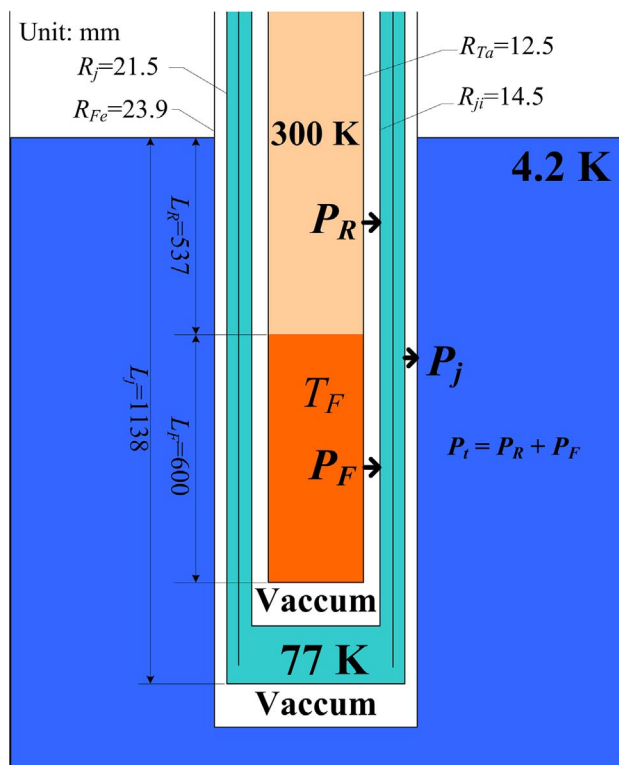


Fig. 5. Schematic of radiation analysis.

through the SSR. Another relay is used to convert the signal from the controller to the temperature setting device: each time the controller sends a pulse, the set temperature is increased by 1 °C. The greatest magnetic field induced by the current in Ni-Cr wire occurs at the

bottom of the heater, the value is about  $4 \times 10^{-4}$  T when the current reaches its limit (10 A). This weak magnetic field won't have apparent effect on the samples in most applications. In earlier experiments using 50 Hz AC heating, the heating wire was cut into two segments at high magnet fields; DC heating has since been applied.

#### 4. Radiation shielding analysis

The second tube absorbs almost all the radiation energy from the tantalum tube (Fig. 5). With LN<sub>2</sub> flowing continuously in area between the second and fourth tube, the radiation heat exchange between the tantalum tube and LHe is cut off. This helps the magnet to work steadily. How much radiation energy does the flowing LN<sub>2</sub> absorb from the tantalum tube? The answer will help to explain the necessity of this radiation-shielding structure. Quantitative analysis for this is showed in the rest of this part.

The radiation power,  $P$ , of two coaxial cylinders can be calculated by the following formula:

$$P = S_1 C_0 (T_1^4 - T_2^4) / [1/\varepsilon_1 + (11/\varepsilon_2) S_1/S_2], \quad (1)$$

where  $\varepsilon_1$  and  $\varepsilon_2$  are the emissivity values,  $S_1$  and  $S_2$  are surface areas,  $C_0 = 5.67 \times 10^{-8} \text{ W K}^{-4} \text{ m}^{-2}$ .

To estimate the radiation and its influence on running the furnace in LHe environment, the radiation power received by the inner surface of outermost tube at 4.2 K is marked as  $P_j$ . Radiation from the bottom of the fourth tube was omitted because their area is relatively negligible, so we have  $P_j = 0.004 \text{ W}$ . According to the value of  $P_j$ , we can deduce that the liquid helium consumption rate attributed from the radiation is 0.0002 g/s, which is about 150 times lower than the normal rate of 0.03 g/s when there is no equipment in the magnet. In conclusion, the radiation load is not affected by the furnace temperature, and its value is too small to cause problems when the equipment is put into the LHe Dewar of the magnet.

The radiation from the tantalum to the second tube can be marked

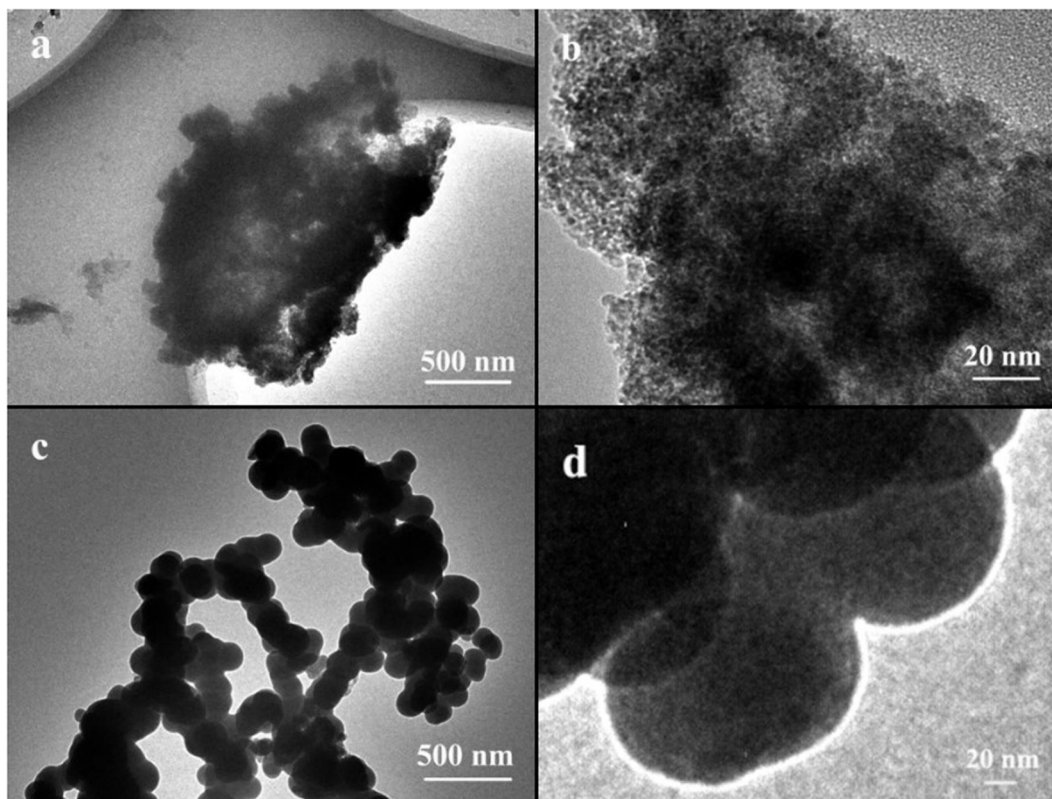


Fig. 6. Transmission electron micrographs of the products prepared (a, b) without the magnetic field and (c, d) within 15 T magnetic field.

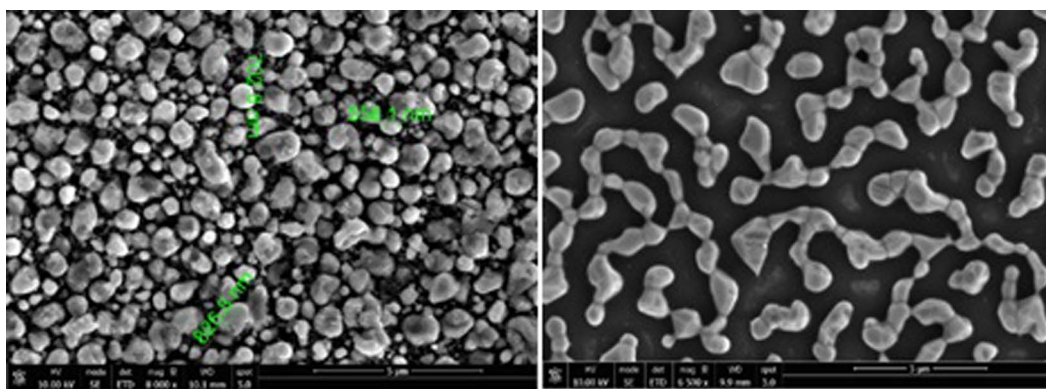


Fig. 7. Scanning electron micrographs of amorphous Co treated at 900 °C (a) without the magnetic field and (b) within 6.8 T magnetic field.

as  $P_t$ . Temperatures of the different parts of the tantalum tube is not a constant when the furnace is heated. A simplified model helps to make quantitative calculation possible. This model assumes that the bottom part of the tantalum tube is at the same temperature as the heater. The upper part of the tantalum is at room temperature, so  $P_t = P_R + P_F$ , where  $P_R$  is a constant and  $P_F$  is mainly decided by temperature of the furnace. From dimension data and formula (1), we have:  $P_t$  (300 K) = 0.88 W;  $P_t$  (500 K) = 6.4 W;  $P_t$  (900 K) = 78 W;  $P_t$  (1200 K) = 278 W. If the  $P_t$ (1200 K) is received by the outermost tube directly, its contribute to the consumption rate of helium will be 13 g/s. This rate is unacceptable for long-time running.

From all above, we can conclude that the LN<sub>2</sub> jacket is essential for longtime running of the furnace.

## 5. Results and discussion

Two applications were made to confirm the two most important aspects of the furnace performance: strong magnetic field compatibility and maximum safe temperature. In the first application, 0.012 g cobalt acetylacetonate and 2 mL oleylamine was dissolved in 2 mL ethanol to prepare the sample. A magnetic field of 15 T was applied. The sample was then heated to 200 °C at 1 °C/min and held for 4 h in an argon atmosphere. For comparison, a control experiment was carried out without applying the magnetic field. Fig. 6(a) and (b) show transmission electron microscopy (TEM) images of the product prepared in the absence of the magnetic field. The product comprised many uniform nanoparticles with an average diameter of about 2 nm. The product produced under the influence of the 15 T superconducting magnet was totally different, as shown by the TEM images of Fig. 6(c) and (d). This product had a much larger size of 150 nm. Interestingly, the nanoparticles had a tendency to connect with each other to form a special necklace-type structure, which may result from the effect of the magnetic field. This application confirmed our furnace is compatible with a magnetic field as strong as 15 T.

In the other application, 200 nm amorphous cobalt film sample on silicon substrate was treated in the furnace. A 6.8 T magnetic field vertical to the sample surface was applied. Then the sample was heated to 900 °C at 10 °C/min and held for 30 min in an argon atmosphere. A control experiment was carried out without the 6.8 T magnetic field. Scanning electron micrographs of the treated amorphous Co samples are shown in Fig. 7. The cobalt particles also had a tendency to contact with each other in the magnetic field.

Additional tests were made to determine the measure error of the temperature and the maximum safe temperature below which longtime running is safe for the magnet. Our laboratory-made thermocouple has a measuring error of less than 1 °C below 200 °C and 4 °C below 900 °C, when compared with a commercial K-type thermocouple. In the process of maintaining a constant temperature, the temperature control system is able to limit the temperature variability to less than 0.1 °C. When the

furnace is cooled or heated, the temperature overshoots by less than 2 °C if the rate of temperature change does not exceed 5 °C/min. To achieve these results, the voltage of the DC power (Fig. 4) must be manually adjusted carefully. The average temperature gradient in the long empty corundum tube was about 0.2 °C/cm when tested at 200 °C. In 900 °C high-temperature experiments, the LN<sub>2</sub> consumption rate was about 20 g/s. The rate was about 5 g/s at 600 °C. But for temperature below 200 °C, the rate was too slow to estimate. With the volume of LN<sub>2</sub> Dewar is 200 L, it is safe for the magnet when the furnace is held at 940 °C not more than 30 min. We are sure that the running time can be prolonged when a Dewar with larger volume is applied. In the 900 °C application experiment, the consumption rate of LHe in the magnet Dewar was as low as 0.04 g/s. As the first application experiment proved that the furnace is compatible with strong magnetic field and the second application checked radiation-shielding performance at 900 °C, the next plan is to apply higher magnetic field (like 18 T) at 900 °C.

## 6. Conclusion

We have developed a high-temperature furnace in 52 mm cold bore magnet. Application experiments have proved its steady performance in strong magnetic field at high temperature. The whole design containing the LN<sub>2</sub> jacket structure has been proved effective in shielding high temperature heat radiation in helium environment. In the future, a LN<sub>2</sub> Dewar with larger volume is planned to be applied. It will be helpful to increase the maximum safe temperature and to prolong the running time at temperature above 900 °C.

## Acknowledgments

This work was supported by the National Key R&D Program of China (Nos. 2016YFA0401003 and 2017YFA0402903), the National Natural Science Foundation of China (Nos. 21505139, 51627901 and 11374278), Anhui Provincial Natural Science Foundation (No. 1608085MB36), the Dean fund of Hefei institutes of Physical Science of CAS (No. YZJJ201620), and Chinese Academy of Sciences Scientific Research Equipment (No. YZ201628).

## References

- [1] Smoluchowski R, Turner RW. *J Appl Phys* 1949;20(8):745–6.
- [2] Mullins WW. Magnetically induced grain boundary motion in bismuth. *Acta Metall* 1956;4(4):421–32.
- [3] Youdelis WV, Colton DR, Cahoon J. On the theory of diffusion in a magnetic field. *Can J Phys* 2011;42(11):2217–37.
- [4] Farrell DE, Chandrasekhar BS, Deguire MR, et al. *Phys Rev B: Condens Matter* 1987;36(7):4025–7.
- [5] Holloway A. *J Appl Phys* 1991;70(10):5716–8.
- [6] Hannay C, Cloots R, Ausloos M. *Solid State Commun* 1992;83(5):349–54.
- [7] Pavard S, Villard C, Bourgault D, et al. Effect of adding MgO to bulk Bi2212 melt

- textured in a high magnetic field. *Supercond Sci Technol* 1998;11(12):1359–66. 8.
- [8] Noudem JG, Beille J, Bourgault D, et al. Bulk textured Bi-Pb-Sr-Ca-Cu-O (2223) ceramics by solidification in a magnetic field. *Physica C* 1996;264(3–4):325–30.
- [9] Bodea S, Vignon L, Ballou R, et al. Electrochemical growth of iron arborescences under in-plane magnetic field: morphology symmetry breaking. *Phys Rev Lett* 1999;83(13):2612–5.
- [10] Wang J, Chen Q, Zeng C, et al. Magnetic-field-induced growth of single-crystalline Fe<sub>3</sub>O<sub>4</sub> nanowires. *Adv Mater* 2004;16(15):22–4.
- [11] Sung MG, Sassa K, Ogawa H, et al. Strengthening of carbon fibers by imposition of a high magnetic field in a carbonization process. *Mater Trans* 2002;43(8):2087–91.
- [12] Wu CY, Murakami Y, Sassa K, et al. Control of crystal orientation of hydroxyapatite by imposing a high magnetic field. *Key Eng Mater* 2005;284–286:75–8.
- [13] Rango PD, Lees M, Lejay P, et al. *Nature* 1991;349(6312):770–2.
- [14] Legrand BA, Chateigner D, Bathie RPD, et al. Orientation by solidification in a magnetic field A new process to texture SmCo compounds used as permanent magnets. *J Magn Magn Mater* 1997;173(1):20–8.
- [15] Sheikh-Ali AD, Molodov DA, Garmestani H. Magnetically induced texture development in zinc alloy sheet. *Scr Mater* 2002;46(12):857–62.
- [16] Shabalin IL. *Ultra-high temperature materials – I*. Netherlands: Springer; 2014. p. 1–6.